Detection and Determination of Depth of Rigid Bottom in Backcalculation of Layer Moduli from Falling Weight Deflectometer Data

A. S. M. MUSTAQUE HOSSAIN AND JOHN P. ZANIEWSKI

A new approach has been developed to detect the presence of a rigid layer at a shallow depth below the pavement using falling weight deflectometer (FWD) deflection data. A parameter, SLOPE, has been derived from the sixth and seventh sensor deflection values by applying Boussinesq's linear elastic idealization to pavement systems under quasi-concentrated FWD load. Typical values of SLOPE have been determined that indicate the presence of a rigid bottom at a shallow depth. The depth of such a rigid layer was determined by matching the outer sensor deflections corresponding to an estimated subgrade modulus with an elastic layer analysis program and a gradient-based optimization routine. The detection and depth determination procedure were verified using FWD measurements, cone penetration results and drilling records on 13 in-service pavements in Arizona, and existing results from manual backcalculation analysis. Satisfactory agreement was observed between the results of this study and results from manual backcalculation analysis. The rigid layer detection and depth determination procedures have been coded in a computer program, Arizona Deflection Analysis Method.

Most backcalculation methods for determination of layer moduli from deflection basins assume a semi-infinite subgrade. McCullough and Taute (*1*) showed that the presence of a rock layer at a finite depth below the pavement can significantly affect theoretical Dynaflect deflection basins. Bush and Alexander (*2*) assumed a rigid bottom at a depth of 240 in. for evaluation of in situ moduli from their deflection basin matching program. Wiseman et al. (*3*) used finite subgrade thickness for their study of nondestructive testing evaluation of pavements. Mamlouk (*4*) and Sebaaly (*5*) arbitrarily selected the depth of the rigid bottom for dynamic analysis of Road Rater, Dynaflect, and falling weight deflectometer (FWD) deflection basins. Uddin et al. (*6*) proposed a method for estimation of the depth of the rigid bottom by dynamic analysis of FWD deflection data. However, no further use of Uddin's method has been reported in the literature. Ullidtz (*7*) reported that ELMOD can detect and estimate the depth of the rigid bottom. Yazdani and Scullion (*8*) reported an experimental program at Texas Transportation Institute using a multidepth deflectometer for monitoring pavement response. A comparison of measured deflections with calculated deflections indicated that a better match was obtained between the two sets when the calculated deflections for the pavement system with a rigid bottom at 240 in. were used.

College of Engineering and Applied Sciences, Arizona State University, Tempe, Ariz. 85287.

Thus, it is apparent that detection and determination of the depth of the rigid bottom, when present at a relatively shallow depth, is an important part of a backcalculation scheme. An approach is presented for the detection of a rigid layer and the estimation of its depth from the top of the subgrade using an FWD deflection basin.

DEFINITION OF RIGID BOTTOM

The rigid bottom, in general, implies the presence of a very stiff layer at some depth below the pavement. In backcalculation, the subgrade is usually characterized as a single uniform layer of infinite thickness in the vertical direction. However, subgrades usually consist of layers of different materials. Mamlouk et al. (*9*) found, through an analysis of cone penetration data on a number of in-service pavement subgrades, that for several of the pavements there was a rigid bottom or "hard rock" basalt or limestone layer underlying the pavement at a finite depth. In most cases the cone penetration data exhibited "medium hard" layers at various depths, sometimes reverting to relatively soft layers beneath the medium hard layers. In a few cases, nothing that could even be called medium hard was encountered within 25 ft of drilling or cone penetration. Figure 1 shows the typical layered profile of subgrade modulus versus depth determined from cone penetration data using the concept of a minimum modulus calculated from cone penetration resistance (*9*). The moduli values were calculated on the basis of correlation among modulus, soil type, and cone tip resistance. The minimum modulus refers to the minimum subgrade modulus encountered in the profile. Figure 1 indicates a remarkable variation of subgrade modulus with depth. Thus, treatment of the subgrade as a single layer in backcalculation requires representing the moduli of several strata in the subgrade with a single composite or equivalent modulus value.

In this study, the rigid bottom refers to the layer in the subgrade in which deformation due to the applied FWD load is essentially zero. The situation might occur because of the presence of an incompressible rock layer or a very hard clay layer in the subsurface. The interface between the subgrade and the rigid layer is considered to be rough (i.e., full continuity exists across such an interface).

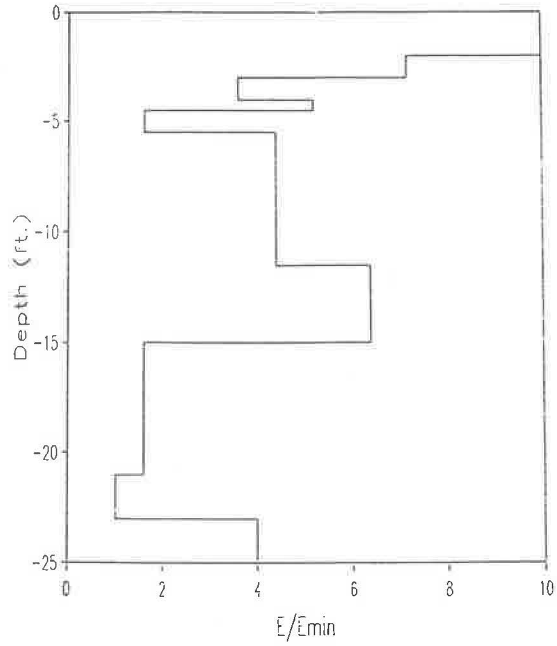

FIGURE 1 Typical layered profile of the subgrade (*9*).

CONSIDERATION OF RIGID BOTTOM IN BACKCALCULATION

The semi-infinite subgrade is an inherent assumption in elastic layer theory for a number of backcalculation processes. For example, the BKCHEVM (*9*) backcalculation program uses CHEVRON (*10*) as the elastic layer analysis program. In this scheme the subgrade is usually assumed to be semi-infinite. However, the BKCHEVM program automatically introduces a rigid bottom 240 in. below the top of the subgrade whenever it detects a rigid bottom on the basis of the seventh sensor deflection value. This detection procedure is arbitrary and not rational.

The BKCHEVM program was used to backcalculate layer moduli for three typical pavements (weak, medium, and stiff) with finite depths of subgrade. Inputs to the program were the simulated deflection basins obtained from CHEVRON for a 9,000-lb load applied on a plate 11.8 in. in diameter on pavements with layer moduli and thicknesses given in Tables 1 and 2. Poisson's ratios of 0.30, 0.40, 0.40, and 0.45 for the asphalt concrete (AC), base, subbase, and subgrade layer materials were assumed.

Tables 1 and 2 show the layer types, thicknesses, and actual and backcalculated layer moduli for different pavement types with finite and infinite depth of subgrade, respectively. Table 1 indicates that the differences between the BKCHEVM-backcalculated and known layer moduli for different layers vary from 14 to 167 percent for pavements with finite depth of subgrade. Table 2 indicates that for infinite depth of subgrade, the differences between backcalculated and known layer moduli are relatively small. For medium and weak pavements, the differences range only from 0.0 to 7.0 percent, whereas for stiff pavement, a 100 percent difference was encountered. Thus, it is evident that for infinite depth of subgrade,

TABLE 1 COMPARISON OF KNOWN AND BACKCALCULATED LAYER MODULI FOR PAVEMENTS WITH FINITE DEPTH OF SUBGRADE

Pavement Type	Layer/ Type[1]	Thickness (in)	Known Modulus (ksi)	Seed Modulus (ksi)	Backcalc. Modulus (ksi)	Diff.[2] (%)
Weak	1/AC	3.0	250	350	70	72.0
	2/AB	4.0	20	40	44	-120.5
	3/SM	9.0	10	30	7	30.0
	4/SG	240	5	8.6	6.7	-33.6
Medium	1/AC	4.0	450	350	100	77.8
	2/AB	4.0	30	40	80	-166.7
	3/SM	12.0	20	30	17.2	14.1
	4/SG	240	10	16.5	13.6	-36.1
Stiff	1/AC	6.0	650	350	1,000	-53.9
	2/AB	4.0	40	40	80	-100.0
	3/SM	9.0	25	30	10	60.0
	4/SG	120	7	20.2	13.2	-88.7

[1] AC: Asphalt Concrete, AB: Aggregate Base, SM: Select Material, SG: Subgrade.
[2] Diff (%) = (Eknown - Ebackcalc)/Eknown x 100

TABLE 2 COMPARISON OF KNOWN AND BACKCALCULATED LAYER MODULI FOR PAVEMENTS WITH INFINITE DEPTH OF SUBGRADE

Pavement Type	Layer/ Type[1]	Thickness (in)	Actual Modulus (ksi)	Seed Modulus (ksi)	Backcalc. Modulus (ksi)	Diff.[2] (%)
Weak	1/AC	3.0	250	350	235.8	6.0
	2/AB	4.0	20	40	21.4	7.0
	3/SM	9.0	10	30	10	0.0
	4/SG	s-i	5	4.99	5	0.0
Medium	1/AC	4.0	450	350	450.4	0.08
	2/AB	4.0	30	40	30.1	0.33
	3/SM	12.0	20	30	19.9	0.50
	4/SG	s-i	10	9.6	10.0	0.00
Stiff	1/AC	6.0	650	350	591.1	9.06
	2/AB	4.0	40	40	80	100.0
	3/SM	9.0	25	30	17.8	28.8
	4/SG	s-i	7	6.8	7.1	2.1

s-i; semi-infinite subgrade

[1] AC: Asphalt Concrete, AB: Aggregate Base, SM: Select Material, SG: Subgrade.
[2] Diff (%) = (Eknown - Ebackcalc)/Eknown x 100

BKCHEVM can predict layer moduli with reasonable accuracy for weak and medium pavements.

Jung (*11*) has shown that the accuracy in the calculation of the moduli of the layers above the subgrade is not important as long as the combined effect of the moduli in transmitting forces to the subgrade remains unchanged. To verify the response of the pavement at the critical location, horizontal tensile strain was calculated with CHEVRON at the bottom of the AC layer corresponding to an 18-kip axle load and 100-psi tire pressure for the known and backcalculated pavement systems. Table 3 shows the comparison of tensile strains calculated at the bottom of the AC layer for known and backcalculated pavement layer moduli for different pavement types and subgrade conditions. The table also shows the number of 18-kip equivalent single-axle loads (ESALs) to be carried by the pavement before fatigue failure, computed from the fatigue criteria developed by Mamlouk et al. (*9*):

$$N = 9.33 \times 10^{-7} (1/e_{ac})^{3.84}$$

where N is the theoretical number of 18-kip ESAL repetitions until fatigue failure and e_{ac} is the tensile strain at the bottom of the AC layer (in microinches per inch).

It is evident that the difference between the asphalt strain corresponding to known layer moduli and the asphalt strain corresponding to backcalculated layer moduli was smaller for infinite depth of subgrade. Consequently, the number of 18-kip ESALs to be carried by the backcalculated pavement systems before fatigue failure does not vary widely from values corresponding to known layer moduli. The maximum difference of 14 percent was for stiff pavement. For finite subgrades, however, the differences between the strain corresponding to backcalculated layer moduli and the strain corresponding to known layer moduli vary from 30 to 49 percent. The differences are magnified when the number of 18-kip ESALs that can be carried by the pavements is computed by using the fatigue criteria developed by Mamlouk et al. (*9*). The differences in computed traffic range between 288 and 1,249 percent. The large differences are attributable to the error resulting from inaccurate determination of the thickness of the subgrade. Detection and accurate prediction of the depth of rigid bottom are important prerequisites for a better backcalculation scheme.

DETECTION OF RIGID BOTTOM

Ullidtz (*7*) has shown that at distances larger than twice the load radius, a distributed uniform load may be treated as a point load. Then, by using Boussinesq's equation, the surface modulus or the "weighted mean modulus" of the elastic half-space idealization of the pavement system can be computed from the surface deflections:

$$E_{sm}(0) = 2(1 - \nu^2)\sigma a/d(0) \quad (1)$$

and

$$E_{sm}(r) = (1 - \nu^2)\sigma a^2/[rd(r)] \quad (2)$$

where

$E_{sm}(r)$ = surface modulus at distance r from the center of the loading plate,
ν = Poisson's ratio (0.35),
σ = contact stress under the loading plate,
a = radius of the loading plate,
$d(r)$ = deflection at distance r, and
r = radial distance from the center of the loading plate.

The surface modulus at distance r roughly reflects the surface modulus at the equivalent depth. In FWD testing, it is assumed that the outermost deflections (sixth and seventh sensors at 12-in. spacing of sensors) are completely controlled by the subgrade. Therefore, the computed surface moduli corresponding to these sensor deflections reflect the contribution of the subgrade. According to Ullidtz (*7*), if the surface moduli (E_{sm6} and E_{sm7}) calculated at the sixth and seventh sensor locations are identical, the subgrade response is linear, that is,

$$\text{SLOPE} = (E_{sm7} - E_{sm6})/E_{sm7} \times 100 \approx 0 \quad (3)$$

This equality implies that the response of subgrade material is linear with depth and that there is no rigid layer at a shallow depth. But if $(E_{sm7} - E_{sm6})/E_{sm7} \times 100 \neq 0$, the response is nonlinear. The nonlinearity might occur because of the nonlinear behavior of subgrade material, the presence of a rigid layer at a shallow depth, or both.

The subgrade material is generally known to be nonlinear (*12*). But it is hypothesized that if the applied load is repeated several times, the effect of nonlinear response due to the

TABLE 3 COMPARISON OF AC STRAIN AND NUMBER OF 18-KIP ESALs CORRESPONDING TO KNOWN AND BACKCALCULATED LAYER MODULI FOR DIFFERENT PAVEMENT TYPES AND SUBGRADE THICKNESSES

Pavement Type	Subgrade Type	Known Strain (micro in/in)	Backcalc Strain (micro in/in)	Diff* (%)	Nknown (millions)	Nbackcalc (millions)	Diff* (%)
Weak	Finite	739.0	375.97	49.12	0.98	13.23	-1249
	Infinite	739.0	730.04	1.2	0.98	1.03	-5.10
Medium	Finite	354.3	235.33	33.58	16.6	80.00	-382.0
	Infinite	354.3	356.57	-0.64	16.6	16.20	2.41
Stiff	Finite	186.73	131.2	9.73	194.3	753.1	-287.6
	Infinite	186.73	170.42	8.73	194.3	166.8	14.41

* Diff (%) = (Known-Backcalc)/Known x 100

subgrade material will be reduced. Kasianchuck and Argue (*13*) showed that the nonlinear load-deflection behavior of a subgrade during the initial loading of a repeated plate load test becomes linear when the load is repeated (Figure 2). This is evidence that the stress-strain behavior of the subgrade becomes linear after repeated traffic loadings.

Mamlouk et al. (*9*) studied the material nonlinearity and stress sensitivity due to FWD loads of the materials of several in-service pavements in Arizona. They found that within the stress range of the FWD tests, the effect of material nonlinearity is negligible compared with the effect of spatial variability in material properties. In other words, the "error" in an FWD deflection measurement resulting from assuming linearity would be insignificant compared with random variability for the subgrades studied. However, for this study the behavior of subgrade and pavement materials was assumed to be linear and elastic. Even with these assumptions, the nonlinearity in the subgrade response due to the presence of a rigid layer at a shallow depth can be significant. Figure 3 shows the effect of the presence of a rigid layer at a shallow depth on the surface moduli for different categories of pavements with assumed linear subgrade material. The effect of the presence of a rigid layer decreases as the depth of the rigid layer increases. At a certain depth, the rigid layer no longer influences pavement response. This critical depth varies with the pavement stiffness.

Table 4 shows the values of SLOPE for linear subgrade material corresponding to different depths of the rigid layer. It is evident that for all pavement types, as the depth of the rigid layer increases, SLOPE decreases. For shallow rigid layers and very stiff pavements, SLOPE becomes negative. The negative SLOPE value implies a positive nonlinearity of the subgrade response, and it happens often with thick pavement structures in which the FWD sensors are too close to the load. This was observed by Ullidtz (*7*). For a very deep layer, SLOPE should be zero (Figure 4). SLOPE values for different pavements vary depending on the thickness and moduli of the layers, especially the subgrade modulus.

Figure 5 shows the relationships between SLOPE and depth of rigid layer for different subgrade moduli for a medium stiff pavement. It is evident that the same pavement has different SLOPE values corresponding to a single depth of rigid layer but different subgrade moduli. Thus, the SLOPE value is a nonunique parameter for detection of a rigid layer, because it is also affected by the subgrade modulus. However, it is possible to develop typical values of SLOPE to detect the rigid bottom empirically.

Table 5 shows the matrix of pavements used in the analysis. The matrix has eight factors each at three levels, yielding $3^8 = 6,561$ pavement structures. These structures were used to generate values of SLOPE for different pavement types with semi-infinite subgrade. A calculated SLOPE from any FWD basin falling outside this range would be attributed to the presence of a rigid layer at a relatively shallow depth. To generate simulated deflection basins, a uniform circular loading of 9,000 lb with a diameter of 11.8 in. was used. Deflections were calculated with CHEVRON (*10*) at the load center and at six other locations at a uniform spacing of 12 in.

SLOPE for each pavement was calculated from Equation 3. Pavements with a subgrade modulus of 3,000 psi were excluded from the analysis because none of the pavements in Arizona analyzed by Mamlouk et al. (*9*) has subgrade modulus

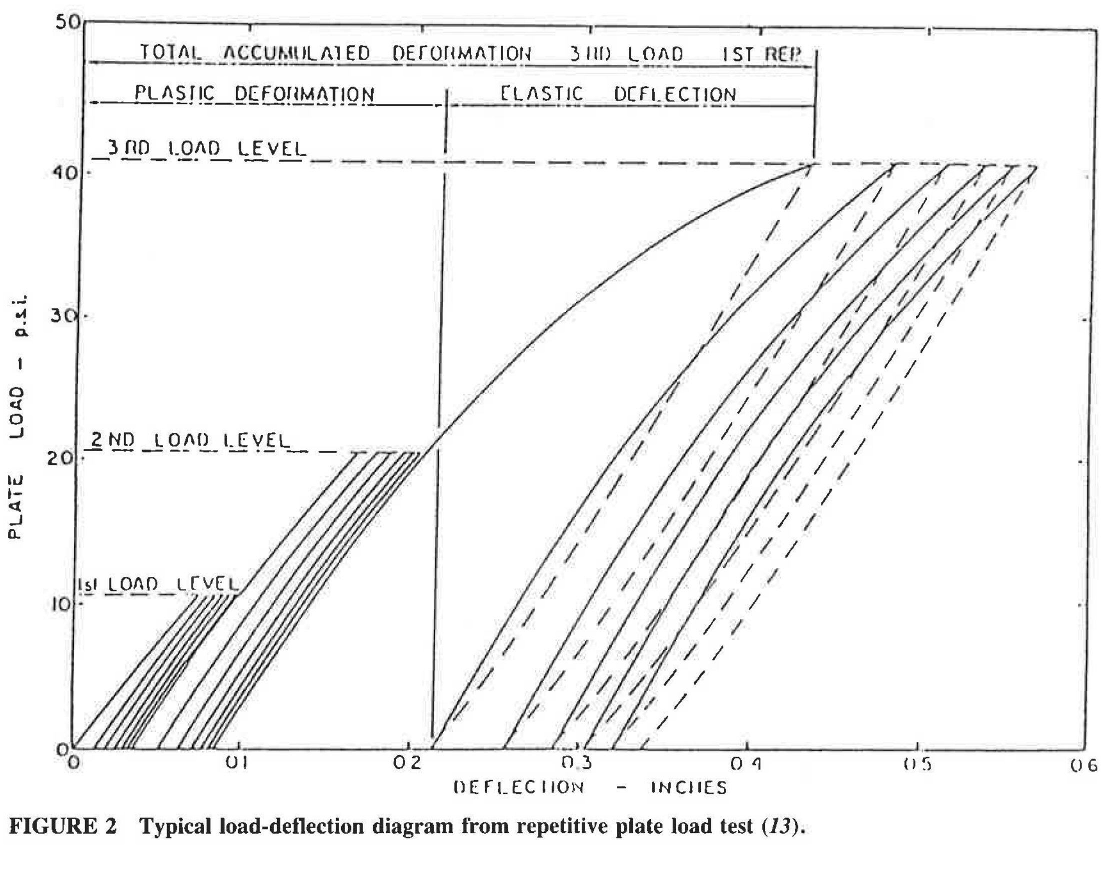

FIGURE 2 Typical load-deflection diagram from repetitive plate load test (*13*).

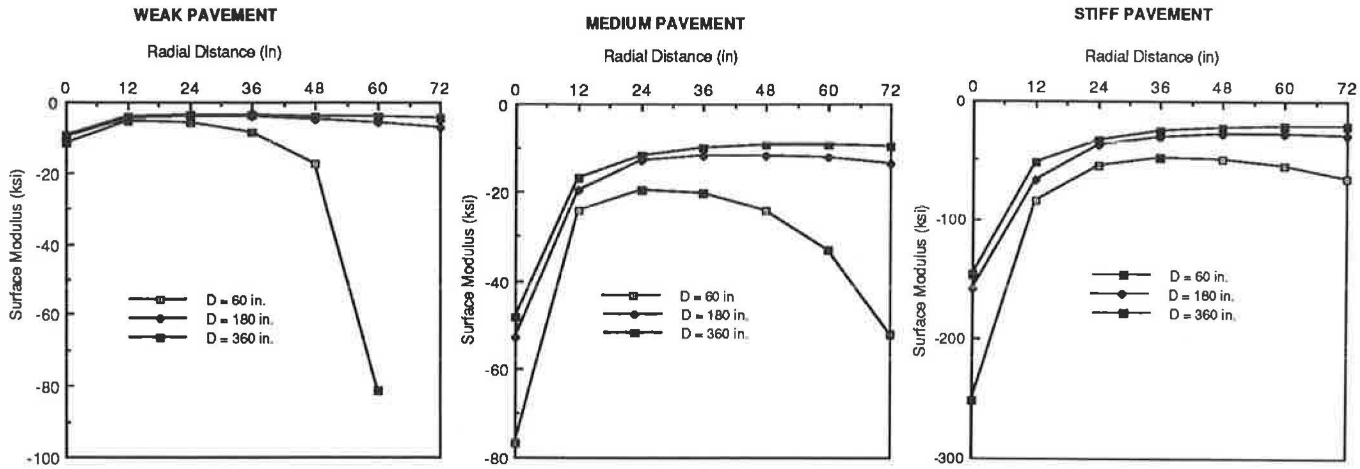

FIGURE 3 Effect of the presence of a rigid layer on the surface moduli of different types of pavements.

TABLE 4 VALUES OF SLOPE FOR DIFFERENT PAVEMENT TYPES AND DEPTHS OF RIGID LAYER

Pavement Type	D[1](inch)	SLOPE(%)
Weak	60	
(3" AC)	120	33.16
	180	18.98
	240	13.74
	300	11.02
	360	9.38
Medium	60	36.7
(7" AC)	120	15.91
	180	9.3
	240	6.26
	300	4.45
	360	3.58
Stiff	60	16.3
(14" AC)	120	6.56
	180	2.55
	240	0.35
	300	-1.19
	360	-1.63

[1] Depth to the rigid layer.

less that 6,500 psi and because the frequency analysis of the seventh sensor deflections from FWD measurements on the Arizona highway system indicated stiffer subgrades for Arizona (*14*). Table 6 shows the summary statistics for SLOPE for different pavement types. On the basis of the range of values in Table 6, the following guidelines were selected to indicate semi-infinite subgrade or linear subgrade response:

For 3 in. $\leq T_{AC} <$ 6 in., $0.22 \leq$ SLOPE < 4.47

For 6 in. $\leq T_{AC} <$ 10 in., $-0.65 \leq$ SLOPE < 7.27

For 10 in. $\leq T_{AC}$, $-3.16 \leq$ SLOPE < 7.80

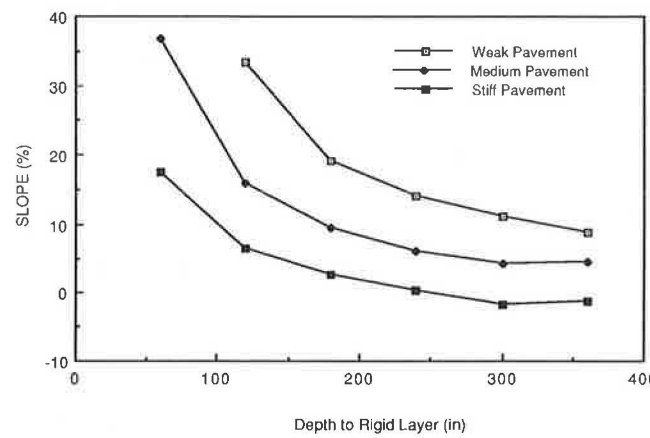

FIGURE 4 Influence of depth of rigid layer on SLOPE for different types of pavements.

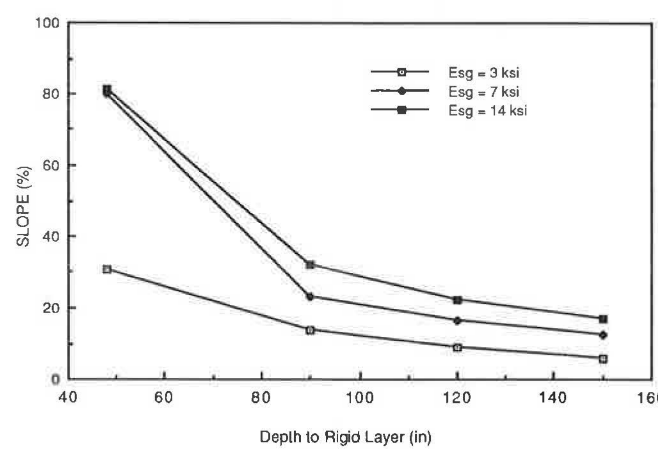

FIGURE 5 Relationship between SLOPE and depth of rigid layer for different subgrade moduli for medium stiff pavement.

For any pavement, if the SLOPE calculated from the sixth and seventh sensor deflections in FWD testing falls outside these ranges, there must be a rigid layer below the pavement at a shallow depth. The presence of this layer makes the subgrade response nonlinear, as the SLOPE value shows.

TABLE 5 PAVEMENT MATRIX USED FOR SIMULATED DEFLECTION BASIN GENERATION

LEVELS	FACTORS							
	T_{AC} (in)	T_{AB} (in)	T_{SM} (in)	D (in)	E_{AC} (ksi)	E_{AB} (ksi)	E_{SM} (ksi)	E_{SG} (ksi)
(1) LOW	3.0	4.0	9.0	120	100	15	10	3
(2) MED	6.0	4.0	12.0	240	450	30	20	7
(3) HIGH	10.0	6.0	18.0	s-i	850	50	30	14

Note: 1) D: Depth to Rigid Layer, s-i: semi-infinite subgrade

2) AC: Asphalt Concrete, AB: Aggregate Base, SM: Select Material/ Subbase, SG: Subgrade

TABLE 6 SUMMARY STATISTICS FOR SLOPE FOR PAVEMENTS WITH SEMI-INFINITE SUBGRADE

Pavement Type	Statistic	SLOPE
Weak (3"AC)	Mean	2.83
	Std. Dev.	0.807
	C.V.(%)	37.0
	Range	0.22 - 4.47
Medium (6"AC)	Mean	3.41
	Std. Dev.	1.40
	C.V.(%)	64.0
	Range	-0.65 - 7.27
Stiff (10"AC)	Mean	2.69
	Std. Dev.	2.24
	C.V.(%)	101.0
	Range	-3.16 - 7.8

However, a negative SLOPE value should be treated with caution. Positive nonlinearity, evident from the negative SLOPE value, might indicate that the pavement is too stiff to apply the "surface modulus" concept and that the remote deflection sensors should be moved further away from the load.

VERIFICATION WITH FIELD DATA

The recommended values of SLOPE for detection of a rigid bottom were tested by using FWD deflection data for the Arizona pavements given in Tables 7 and 8. Table 9 shows the results of the analysis. The method accurately predicted the presence of a rigid layer in almost all cases. Of the 22 deflection basins evaluated, 19 were correctly classified with respect to the rigid bottom determination. This is acceptable

TABLE 7 TEST SITES AND PAVEMENT TYPES

Site	Location	Route	Mile Post	Pavement Type
1	Benson	I10W	300.07	5-layer
3	Winslow	I40E	260.21	4-layer
4	Minnetonka	I40E	261.78	4-layer
5	Dead River	I40E	317.06	4-layer
6	Flagstaff	I17N	337.00	4-layer
7	Crazy Creek	I40E	323.78	4-layer
9	Sunset Point	I17N	251.41	5-layer
10	Seligman	I40W	131.71	4-layer
12	Benson East	I10W	303.00	4-layer
14	Jacob Lake	US89AN	578.00	4-layer
18	Morristown	US60W	120.00	4-layer
19	McNary	US260E	369.00	5-layer
20	Kingman	I40E	59.00	4-layer

because of the empirical nature of the approach. Site 7/1 was identified as having semi-infinite subgrade, and the depth of the rigid layer computed by manual matching was 300 in. Because this pavement has an AC thickness of 8.0 in. with a 6-in. cement-treated base, 300 in. of subgrade can be interpreted as a semi-infinite subgrade.

DETERMINATION OF DEPTH OF RIGID BOTTOM

As defined earlier, the depth of the rigid layer refers to the depth of a stiff layer below the subgrade. The subgrade modulus is assumed to reflect the composite modulus or equivalent

TABLE 8 LAYER TYPE AND THICKNESS AT DIFFERENT SITES

Site/ Sta	Layer 1		Layer 2		Layer 3		Layer 4		Layer 5	
	Mat	Thk (in)	Mat	Thk (in)	Mat	Thk (in)	Mat	Thk (in)	Mat	Thk (in)
1/1	AC	7	BS	2.5	AB	2	SB	12	SC-SM*	
3/1	AC	12	BTB	3	SB	5	SM*	-	-	-
4/1	AC	11.5	BTB	2	SB	3	SM*	-	-	-
5/1	AC	8	CTB	4.5	SB	7	SM*	-	-	-
6/1	AC	9	AB	4	SB	12	-	-	-	-
7/1	AC	8	CTB	6	SB	6	SM*	-	-	-
9/1	AC	6	BS	4	SB	26	SGS	6	CL-CH*	-
10/1	AC	6	AB	6	SB	24	CH*	-	-	-
12/1	AC	6	AB	6	SB	18	SC-SM* -	-	-	
14/1	AC	9	BS	4	AB	4	SC-CH* -	-	-	
18/1	AC	4.25	AB	4	SB	15	-	-	-	-
19/1	AC	4.8	BS	2.2	AB	3	SB	6		
20/1	AC	9.5	AB	4	SB	15	-	-		

* Subgrade Classification based on Unified Method.

Note: AC: Asphalt Concrete, BS: Bituminous Surface, BTB: Bituminous Treated Base, CTB: Cement Treated Base, AB: Aggregate Base, SGS: Subgrade Seal, SB: Sub Base (Select Material)

TABLE 9 RESULTS OF USING SLOPE TO DETECT RIGID BOTTOM (FWD DEFLECTION DATA)

Site/Sta	T_{AC}(in)	SLOPE(%)	Rigid Bottom[1]	D[2](in)
1/1	7.0	10.00	YES	140
3/1	12.0	-7.37	YES	S.inf
3/7	12.5	2.86	NO	S.inf
4/1	11.5	2.86	NO	S.inf
5/1	8.0	20.00	YES	85
5/4	8.0	17.89	YES	82
6/1	9.0	20.00	YES	60
7/1	8.0	3.23	NO	300
7/4	6.25	0.69	NO	S.inf
9/1	6.0	15.29	YES	72
10/1	6.0	12.70	YES	S.inf
10/7	6.5	0.80	NO	S.inf
12/1	6.0	7.69	YES	100
14/4	9.0	7.57	YES	120
18/1	4.25	0.0	NO	S.inf
18/4	4.25	6.15	YES	120
19/1	4.8	8.15	YES	240
19/4	4.8	10.93	YES	240
20/1	9.5	-2.58	YES	150

[1] Rigid bottom detected based on the value of SLOPE

[2] Values are after Mamlouk et al, (9)

modulus of the materials between the bottom of the pavement structure and the rigid layer. The moduli of the pavement layers above the subgrade do not contribute much toward the deflections measured at the outermost sensors (*7*). Again, deflections at the sixth and seventh sensor locations calculated from elastic layer theory are highly affected by the presence of a rigid layer at a shallow depth, as shown in Table 10. Thus, when finding the depth of rigid layer corresponding to an equivalent subgrade modulus, estimated values from regression equations can be assigned to the upper layer moduli (*14*).

The thickness of subgrade can be found by minimizing the error between the measured and calculated deflection values at the sixth and seventh sensor locations. An objective function can be defined as

$$\text{minimize } f = \sum_{i=1}^{n} W_i[(\Delta_i^m - \Delta_i^c)/\Delta_i^m]^2 \tag{4}$$

with

$$D^L \leq D \leq D^U$$

where

- f = squared error,
- W_i = weighting factor for Sensor i (1 for Sensor 6 and 2 for Sensor 7),
- Δ_i^m = measured deflection at Sensor i,
- Δ_i^c = calculated deflection at Sensor i,
- D = thickness of the subgrade,
- D^L = lower limit of thickness of the subgrade,
- D^U = upper limit of thickness of the subgrade, and
- n = number of sensors = 2 (i.e., the sixth and seventh).

TABLE 10 EFFECT OF RIGID BOTTOM ON SIMULATED DEFLECTION VALUES

Pavement Type	D (in.)	Difference in Deflections for Sensor No.(%) 1	2	3	4	5	6	7
Weak	360*	0	0	0	0	0	0	0
	180	6	9	8	15	22	29	37
	60	20	26	40	59	78	95	-
Medium	360*	0	0	0	0	0	0	0
	180	9	15	9	15	20	24	29
	60	37	31	40	51	62	72	82
Stiff	360*	0	0	0	0	0	0	0
	180	8	23	10	15	21	24	27
	60	42	39	36	47	55	61	68

* Deflections corresponding to D = 360 in. have been taken as standards.

Equation 4 can be rewritten as

$$\text{minimize } f = \sum_{i=1}^{n} W_i(1 - \Delta_i^c/\Delta_i^m)^2 \tag{5}$$

with

$$D^L \leq D \leq D^U$$

Equation 5 is minimized by OPTECH (*15*), a powerful and efficient gradient-based technique for constrained nonlinear function optimization that converges rapidly and uses both function and gradient of the function information.

Because the effect of subgrade modulus on the sixth and seventh sensor deflection values is significant, an accurate estimation of subgrade modulus is required before calculating the thickness of the subgrade or depth of the rigid layer. Two approaches were investigated for estimating the equivalent subgrade modulus: (*a*) empirical study of simulated deflection basins and (*b*) correlation with the resistance or *R* values of subgrade soils determined in the laboratory (AASHTO T190).

Empirical Study of Simulated Deflection Basins

Uddin et al. (*6*) estimated the subgrade modulus from the fifth sensor deflection of the Dynaflect, and Ullidtz (*7*) estimates subgrade modulus with the seventh sensor deflection value of the Dynatest FWD, which is valid only for semi-infinite subgrade. Because the deflection value measured by the seventh sensor is very small in magnitude, a small variation in measurement at this location results in a large error in the estimation of subgrade modulus (*7*). In this study, an exponential curve of the form $Y = Ae^{BX}$ was fitted to deflection basins consisting of all seven sensor deflections. Y is the deflection in mils, and X is the radial distance from the load in inches. A and B are the regression constants that define the shape of the deflection basin (*14*). The A and B values were computed over 6,000 simulated deflection basins from elastic layer analysis, and regression equations were developed for estimating subgrade modulus from A and B. Because, depending on the pavement type, 70 to 95 percent of the total surface deflections are contributed by the subgrade layer (*12*), the estimation of subgrade modulus from the parameters A and B is more rational than using a single sensor deflection value.

The pavements used in the development of regression equations for subgrade modulus were those described in Table 5. Separate equations were developed for subgrades with finite and infinite thickness. The equations were developed by stepwise forward multiple linear regression using STATPAK (*16*). The logarithm of the subgrade modulus was the dependent variable, and A and B were the independent variables. A log transformation of A was used to achieve linearity in the relationship.

The equation for pavements with finite subgrade thickness is

$$y = 4.508 - 0.986\log_{10}A - 19.896B \qquad R^2 = 0.89$$

$$\text{Esubgrade} = 10^y \qquad n = 4{,}374 \tag{6}$$

For infinite subgrade thickness, the equation is

$$y = 4.639 - 1.019\log_{10}A - 24.467B \qquad R^2 = 0.994$$

$$\text{Esubgrade} = 10^y \qquad n = 2{,}187 \tag{7}$$

Correlation with Laboratory Resistance or *R* Values of Soil

The ADOT *Preliminary Engineering Design Manual* (*17*) estimates the subgrade modulus with the equation

$$\text{Esubgrade} = \frac{[1{,}815 + 225(\text{Rmean}) + 2.40(\text{Rmean})^2]}{0.6(\text{SVF})^{0.6}} \tag{8}$$

In Equation 8, SVF is the seasonal variation factor and

$$\text{Rmean} = \frac{\text{Nt Rt } \sigma c^2 + \text{Nc Rc } \sigma t^2}{\text{Nt}\sigma c^2 + \text{Nc}\sigma t^2}$$

where

- Nt = number of actual *R* values,
- Nc = number of correlated *R* values (from PI and percentage of material passing a No. 200 sieve),
- Rt = mean of the actual *R* values,
- Rc = mean of the correlated *R* values,
- σt = standard deviation of the actual *R* values, and
- σc = standard deviation of the correlated *R* values.

Calculation Scheme

The calculation scheme to find the depth of the rigid layer corresponding to an estimated subgrade modulus is as follows:

1. FWD-measured deflections are normalized to a 9,000-lb load assuming linear response of the subgrade, and an exponential curve of the form $Y = Ae^{BX}$ is fitted to the deflection basin.
2. The subgrade modulus is calculated both by the regression equations involving A and B and the *R*-value approach. The layer moduli of other layers are calculated from appropriate regression equations from Table 11. An initial estimate of subgrade thickness is 240 in.
3. CHEVRON is used to compute the theoretical surface deflection at each sensor location corresponding to the FWD test load, and the objective function (f^{old}) is calculated corresponding to the FWD-measured deflection values.
4. The thickness of the subgrade is perturbed by an amount ΔD, the deflections are again calculated by using CHEVRON, and a new value of the objective function (f^{new}) is computed.
5. The gradient of the objective function is computed by the following formula:

$$\partial f/\partial D = (f^{\text{new}} - f^{\text{old}})/\Delta D$$

6. The gradient and thickness values are fed into an optimization routine (OPTECH), which estimates a new thickness value corresponding to the minimized objective function.

TABLE 11 REGRESSION EQUATIONS FOR ESTIMATING PAVEMENT LAYER MODULI

Layer	Equation for Modulus (psi)	R^2	Ref.
AC	$E = 1{,}377{,}559 - 49{,}389\, t_{ac} - 7{,}868\, t_{sb} - 1.02\, E_{sg} - 25{,}470\, d_1$	0.71	14
(for finite subgrade)			
	$E = -254{,}809 - 13{,}761.5\, t_{ac} + 26.33\, E_{sg} + 12{,}192.54\, d_1$	0.74	14
(for infinite subgrade)			
	$90{,}0000 \le E \le 1{,}500{,}000$		
CTB,	$E = 388{,}522 - 8023\, t_{sb} - 9701\, d_1$	0.74	14
BTB, BS			
	$60{,}000 \le E \le 450{,}000$		
AB	$E = E_{sm}(1 + 10.52 \operatorname{Log}(t_{ab}) - 1.56 \operatorname{Log}(E_{sm}) \operatorname{Log}(t_{ab}))$	-	18
	$10{,}000 \le E \le 2\,E$ (calculated)		
SM	$E = E_{sg}(1 + 7.18 \operatorname{Log}(t_{subbase}) - 1.56 \operatorname{Log}(E_{sg}) \operatorname{Log}(t_{sm}))$	-	18
	$10{,}000 \le E \le 2\,E$ (calculated)		

Note: AC: Asphalt Concrete, BS: Bituminous Surface, BTB: Bituminous Treated Base, CTB: Cement Treated Base, AB: Aggregate Base, SM: Select Material, t: thickness (in); d_1: FWD First sensor deflection (mils).

7. Steps 4 through 6 are repeated until the objective function stabilizes or the calculated thickness value in successive iterations does not change by more than 5 percent. The thickness value corresponding to the minimized objective function is the calculated depth of the rigid bottom.

Figure 6 shows a flowchart of the calculation scheme. This scheme and the rigid layer detection procedure have been coded in the computer program Arizona Deflection Analysis Method (ADAM). Convergence of the objective function usually requires three to five iterations on a Digital VAX 6000-410 machine. A typical rigid bottom detection and determination scheme usually requires 30 to 70 sec of CPU time. The program is coded in ANSI FORTRAN77 and should work on microcomputers.

ANALYSIS WITH FIELD DATA

The procedure for determining the depth of the rigid layer was tested with the FWD deflection data for the sites in Table 7. The subgrade moduli were computed by using Equations 6 or 7 and Equation 8. Table 12 shows the subgrade modulus and the depth of the rigid layer computed by ADAM and by manual matching of the deflection basins (*9*). In most cases the modulus of the subgrade and the depth of the rigid layer determined from *A* and *B* in this study agree well with those computed by manual matching. The calculation scheme developed in this study appears to have captured the "intelligence" in the manual matching of deflection basins.

The subgrade modulus computed from the *R* values of the subgrade soil and the corresponding depth of the rigid layer are not in good agreement with those from manual matching. The modulus of the subgrade is a measure of the elasticity of the material, whereas the *R* value is an index value representing the deformation of the material under certain prescribed conditions. The correlation between the two cannot be expected to be good in all cases, because these properties are not directly related to each other. In addition, the laboratory *R*-value determination is done on a small amount of disturbed subgrade material, whereas the composite subgrade modulus from backcalculation represents a large volume of undisturbed material (*9*).

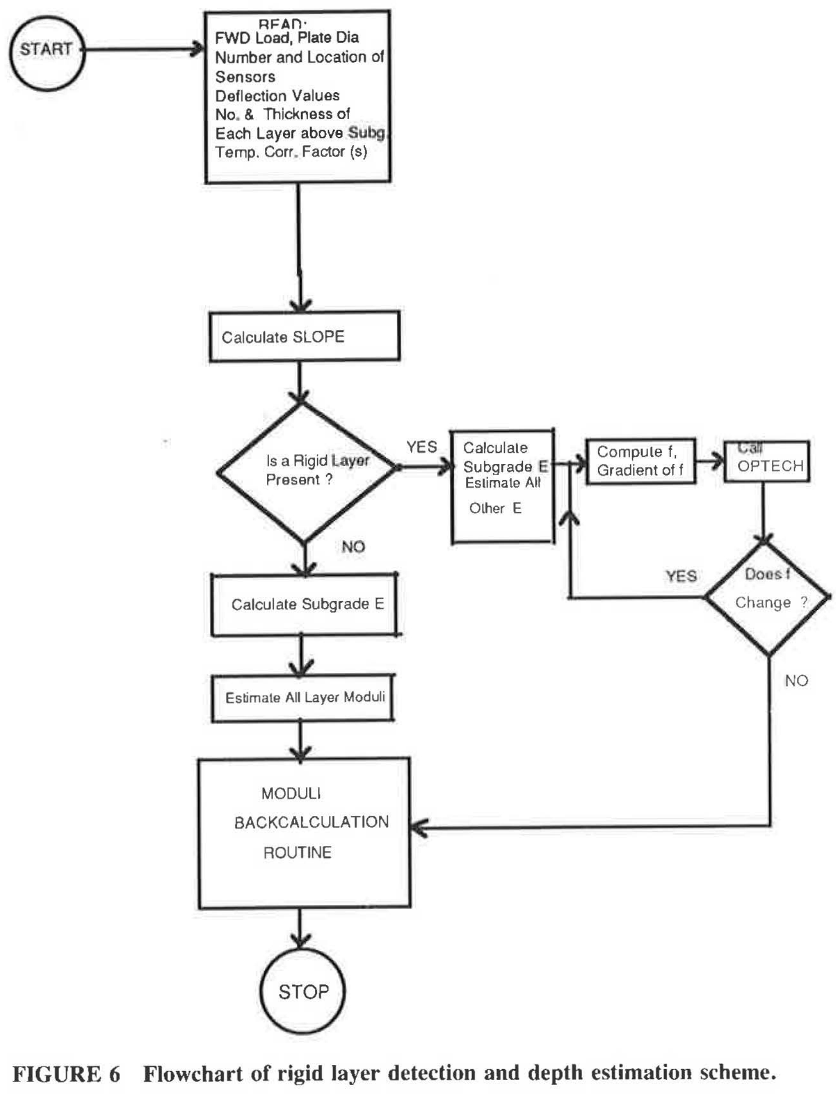

FIGURE 6 Flowchart of rigid layer detection and depth estimation scheme.

TABLE 12 COMPARISON OF SUBGRADE MODULI AND THICKNESSES CALCULATED BY ADAM WITH THOSE COMPUTED FROM MANUAL MATCHING OF DEFLECTION BASINS

Site/Station	Regression Eqn. Esg (ksi)	Regression Eqn. D (in)	"R"-Value Eqn Esg (ksi)	"R"-Value Eqn D (in)	Manual Matching* Esg (ksi)	Manual Matching* D (in)
1/1	18.8	124	20.0	131	18.0	140
3/7	18.4	s-inf	12.2	195	20.0	s-inf
4/1	18.9	s-inf	5.2	69	20.5	s-inf
5/4	12.5	143	31.6	s-inf	7.0	82
6/1	14.8	128	-	-	6.5	60
7/4	12.4	s-inf	20.2	s-inf	13.5	s-inf
9/1	12.0	126	6.6	73	8.5	72
10/4	7.6	165	-	-	10.0	240
10/7	15.9	s-inf	-	-	16.0	s-inf
12/1	13.7	135	22.4	300	10.5	100
14/4	24.9	146	5.7	56	25	120
18/1	48.5	s-inf	30.5	251	50	s-inf
18/4	4.7	150	-	-	22	120
19/1	7.8	150	-	-	10	240
19/4	8.7	150	-	-	11	240
20/1	29.8	127	36.4	150	45	150

* After Mamlouk et al. (9)

TABLE 13 COMPARISON OF CALCULATED DEPTH OF RIGID BOTTOM WITH DRILLING AND CONE PENETRATION RESULTS

Site/ Station	Regr. Eqn. Depth (in)	R-val. Eqn. Depth (in)	Manual* Matching Depth (in)	Drilling & Cone Results** (in)
1/1	124	131	140	Drilling stopped @ 300. Cone Refusal at: >180.
3/7	s-inf	s-inf	s-inf	Drilling stopped @ 300. Cone pen. stopped @ 300.
4/1	s-inf	69	s-inf	Drilling stopped @ 144. Cone pen. stopped @ 144. Presence of Ground Water.
5/4	143	s-inf	82	Drilling stopped @ 300 Cone refusal @ 72.
6/1	128	-	60	None
7/4	s-inf	s-inf	s-inf	Drilling stopped @ 300 Cone refusal @ 120.
9/1	126	73	72	Drilling stopped @ 60 Cone refusal @ 60. Basalt at 60 in.
10/4	165	-	240	Drilling stopped @ 300 Cone refusal @ 144.
10/7	s-inf	-	s-inf	None
12/1	135	300	100	Drilling stopped @ 300. Cone Refusal @ 300 Vry hrd drill: 120-300.
14/4	146	56	120	Drilling stopped @ 90. Cone refused @ 90. Limestone at 90 in.

* After Mamlouk et al. (9)
** After project HPR-PL-1(33) Item 254, Rational Characterization of Pavement Structures Using Deflection Analysis, Arizona Department of Transportation.

Table 13 compares the depths of the rigid layers, or subgrade thicknesses, computed in this study with the drilling and cone penetration test results obtained on several existing pavement subgrades in Arizona (*9*). The manual matching and modulus from the *R*-value approach predicted the existence of a rigid rock layer fairly accurately for Sites 9 and 14. However, when the results of calculations for all the sites are considered, it is evident that no set of calculated depths is in excellent agreement with the drilling and penetration results.

Because both subgrade modulus and thickness determine the surface deflections of the outermost sensors, the ADAM results indicate a compensating effect compared with manual matching. In other words, if the subgrade modulus is lower than the manual matching values, there is a corresponding decrease in subgrade thickness. The subgrade moduli calculated corresponding to *A* and *B* and the corresponding depths of the rigid layer are in good agreement with the manual matching procedure.

SUMMARY

A method has been developed for detection and determination of the depth of a rigid layer from an empirical study of the simulated deflection basins from elastic layer theory. The method uses the outermost sensor deflections from FWD testing. It has been verified with field data and shown to be accurate for practical purposes in predicting the presence of a rigid layer at a shallow depth below the pavement. Agreement with a manual matching method was also observed. On the basis of the algorithm for this method, a computer program, ADAM, was developed for detection and estimation of the depth of a rigid layer. The program has been implemented on a Digital VAX 6000-410 mainframe.

REFERENCES

1. B. F. McCullough and A. Taute. Use of Deflection Measurements for Determining Pavement Material Properties. In *Transportation Research Record 852*, TRB, National Research Council, Washington, D.C., 1982, pp. 8–15.
2. A. J. Bush III and D. R. Alexander. Pavement Evaluation Using Deflection Basin Measurements and Layered Theory. In *Transportation Research Record 1022*, TRB, National Research Council, Washington, D.C., 1985, pp. 16–22.
3. G. Wiseman, J. Greenstein, and J. Uzan. Application of Simplified Layered System to NDT Pavement Evaluation. In *Transportation Research Record 1022*, TRB, National Research Council, Washington, D.C., 1985, pp. 29–36.
4. M. S. Mamlouk. Use of Dynamic Analysis in Predicting Field Multilayer Pavement Moduli. In *Transportation Research Record 1043*, TRB, National Research Council, Washington, D.C., 1985, pp. 113–120.
5. B. E. Sebaaly. *Dynamic Models for Pavement Analysis*. Ph.D. dissertation. Department of Civil Engineering, Arizona State University, Tempe, 1987.
6. W. Uddin, A. H. Meyer, W. R. Hudson, and K. H. Stokoe II. *A Structural Evaluation Methodology for Pavements Based on Dynamic Deflections*. Research Report 387-1. Center for Transportation Research, University of Texas at Austin, Austin, 1985.
7. P. Ullidtz. *Pavement Analysis*. Elsevier, New York, 1987.
8. J. I. Yazdani and T. Scullion. Comparing Measured and Theoretical Depth Deflections Under a Falling Weight Deflectometer Using a Multidepth Deflectometer. In *Transportation Research Record 1260*, TRB, National Research Council, Washington, D.C., 1990, pp. 216–225.
9. M. S. Mamlouk, W. N. Houston, S. L. Houston, and J. P. Zaniewski. *Rational Characterization of Pavement Structures Using Deflection Analysis*. Report FHWA-AZ87-254, Vol. 1. Center for Advanced Research in Transportation, Arizona State University, Tempe, 1988.
10. L. J. Painter. *CHEVRON N-Layer Program—Improved Accuracy*. California Research Corporation, Richmond, Calif., 1980.
11. F. W. Jung. Interpretation of Deflection Basin for Real-World Materials in Flexible Pavements. Presented at 69th Annual Meeting of the Transportation Research Board, Washington, D.C., 1990.
12. E. J. Yoder and M. W. Witczak. *Principles of Pavement Design*, 2nd ed. John Wiley and Sons, Inc., New York, 1975.
13. D. A. Kasianchuck and G. H. Argue. A Comparison of Plate Load Testing with the Wave Propagation Technique. *Proc., 3rd International Conference on the Structural Design of Flexible Pavements*, London, 1972, pp. 444–454.
14. A. S. M. M. Hossain. *Deflection Analysis of Flexible Pavements Using Nondestructive Test Data*. Ph.D. dissertation. Department of Civil Engineering, Arizona State University, Tempe, 1990.
15. S. D. Rajan. *A User's Guide to OPTECH*. Technical Report. Department of Civil Engineering, Arizona State University, Tempe, 1985.
16. *STATPAK User Guide*. Northwest Analytical, Inc., Portland, Oreg., 1983.
17. *Materials Preliminary Engineering Design Manual*, 3rd ed. Arizona Department of Transportation, Phoenix, 1989.
18. J. P. Zaniewski, W. R. Hudson, S. B. Seeds, and L. Moser. *Pavement Performance Model Development*. Report FHWA/RD-84/103, Vol. 2. ARE Inc., Austin, Tex., 1984.